Fault Detection and Isolation Using the Generalized Parity Vector Technique in the Absence of a Mathematical Model

Maira Omana and James H. Taylor

***Abstract*— This paper is an extension of the generalized parity vector (GPV) approach presented in Omana and Taylor [1] and [2]. In the present work, this fault detection and isolation (FDI) technique is implemented on a two-phase separator followed by a three-phase gravity separator model used in oil production facilities. This model simulates a larger scale process, which allows the technique to be tested in a higher dimensional space with more complex system dynamics. Also, the plant model availability issue is overcome by incorporating a system identification module before executing the FDI block. This shows that while the GPV is a model-based technique, it is still viable for FDI even for those plants where only input-output data are available.**

I. INTRODUCTION

Fault detection and isolation (FDI) using the generalized parity vector (GPV) technique is a quantitative model-based approach based on the linearized state space representation. Although quantitative model-based approaches have made an impact in mechanical and aeronautical engineering applications, they have had little impact in process industries [3]. One of the major advantages of using the quantitative model-based approach is that we will have some control over the behavior of the residuals. However, several factors such as system complexity, high dimensionality, process nonlinearity and/or lack of good data often render it very difficult even impractical to develop an accurate mathematical model for the system. This limits the usefulness of this approach in real industrial processes [4].

So far, the GPV technique has been successfully tested using a second-order aircraft engine model [10] and a third-order linearized state-space obtained analytically from the original nonlinear model for a jacketed continuously stirred tank reactor (JCSTR) [1], [2]. In this paper, the viability of the GPV implementation in real industrial processes is analyzed using a gravity three-phase separation process, which allows us to test this FDI method in a higher dimensional space and in a case where a mathematical model is lacking.

This paper is outlined as follows: First, a brief overview of stable factorization and its application to implement the generalized parity vector technique is given in section II. Next, in section III, sensor and actuator FDI using directional residuals are defined [5], [6], [7]. Section IV presents an overview of the transformation matrix optimization method proposed in Omana and Taylor [1] and includes an extension to solve the hyperplane intersection issue. Section V describes briefly the gravity three-phase separation process and its control loops, followed by system identification results in section VI. Finally, section VII present the FDI results obtained using the separator model described in section V for different scenarios.

Maira Omana is a Ph.D. candidate with the Department of Electrical & Computer Engineering, University of New Brunswick, PO Box 4400, Fredericton, NB CANADA E3B 5A3 maira.omana@unb.ca

James H. Taylor is a Professor in the Department of Electrical & Computer Engineering, University of New Brunswick, PO Box 4400, Fredericton, NB CANADA E3B 5A3 jtaylor@unb.ca

II. RESIDUAL GENERATION USING THE GENERALIZED PARITY VECTOR TECHNIQUE

The residual generator is implemented using the generalized parity vector technique, which is developed in the stable factorization framework. The significance of using the stable coprime factorization approach is that the parity relations obtained involve stable, proper and rational transfer functions even for unstable plants. Therefore the realizability and stability of the residual generator is guaranteed. Given any *nxm* proper rational transfer function matrix *P(s)*, it can be expressed in terms of its left coprime factors as follows [8]:

$$P(s) = \tilde{D}(s)^{-1}\tilde{N}(s) \tag{1}$$

where $\tilde{N}(s)$ and $\tilde{D}(s)$ are called the left coprime factors and belong to the set of stable transfer function matrices. The GPV technique is based on the stable factorization of the system transfer function matrix in terms of its state-space representation. Let the system be described by the set of equations:

$$\dot{x}(t) = Ax(t) + Bu(t) \tag{2}$$

$$y(t) = Cx(t) + Eu(t) \tag{3}$$

where x, u, and y represent the state variables, inputs, and outputs of the system, respectively. Assuming that the pairs (A, B) and (A, C) are stabilizable and detectable, it is possible to select a constant matrix F with appropriate dimensions, such that the matrix $A_o \triangleq A - FC$ is stable. Using the definition of the coprime factorization of P(s) in [9], the left coprime factors are given by:

$$\tilde{N} = C(sI - A_o)^{-1}(B - FE) + E \tag{4}$$

$$\tilde{D} = I - C(sI - A_o)^{-1}F \tag{5}$$

Based on the definition of the transfer function matrix *P(s)* given in equation (1) and taking the relationship among the desired control input, u_d, and the actual output of the sensors, *y*, the following relations are obtained:

$$P(s) = \tilde{D}(s)^{-1}\tilde{N}(s) = \frac{y(s)}{u_d(s)} \tag{6}$$

$$\tilde{D}(s)y(s) - \tilde{N}(s)u_d(s) = 0 \tag{7}$$

Under ideal conditions, when the plant is linear, noise and fault free, equation (7) holds. However, when a fault happens, this relation is violated showing the inconsistency between the actuator inputs and sensor outputs with respect to the unfailed model.

Using this fact, the generalized parity vector, ***p(s)***, is defined as:

$$p(s) = T_r\,[\,\tilde{D}(s)y(s) - \tilde{N}(s)u_d(s)\,] \tag{8}$$

The GPV $p(s)$ is a time varying function of small magnitude under normal operating conditions, due to the presence of noise and modeling errors arising from linearization and order reduction. However, it exhibits a significant magnitude change when a fault occurs. Each distinct failure produces a parity vector with different characteristics, allowing the use of the GPV for isolation purposes. A transformation matrix $T_r(s)$ is introduced to make it possible to isolate faults more effectively [10].

III. Fault Detection and Isolation using directional residuals

The basic idea of FDI using failure directions is that each failure will result in activity of the parity vector along certain axes or in certain subspaces. Depending on the dynamics of the system, some of these reference directions may be close or identical, making the isolation for some faults difficult or unachievable. To overcome the angle separation problem between the reference directions, the calculation of an optimal transformation matrix T_r is introduced in section IV.

A. Actuator Faults

Assuming an additive fault $a_j(t)$ in the j^{th} actuator and using the definitions in section II, the GPV becomes:

$$p_{a,j}(s) = -(T_r\tilde{N})^j a_j(s) \triangleq T_r B_n^j \frac{a_j(s)}{s+\sigma} \tag{9}$$

Equation (9) shows that $p_{a,j}(s)$ is restricted to exhibit activity along the direction defined by the j^{th} column of $\tilde{N}$, which we denote B_n^j [10].

Actuator fault isolation is thus based on the angle Θ_j between the GPV and B_n^j as illustrated in figure 1. If the j^{th} actuator is faulty, this angle should be zero in the ideal case or less than a small threshold value, T_h, to account for model uncertainty, noise and/or unknown disturbances. To make the graphical illustration easier, the GPV in figs. 1 and 2 is plotted in a 3-dimensional space. However, for the separator model described in section V the FDI is performed in a 5-dimensional space, which corresponds to the number of input-outputs in the system.

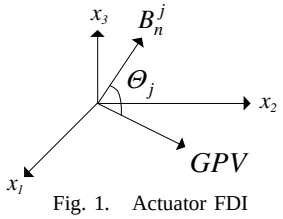

Fig. 1. Actuator FDI

B. Sensor faults

Similarly, for an additive fault $s_i(t)$ in the i^{th} sensor the parity vector in equation (8) reduces to:

$$p_{s,i}(s) = (T_r\tilde{D})^i s_i(s) \triangleq T_r\left[E_d^i + \frac{B_d^i}{s+\sigma}\right] s_i(s) \tag{10}$$

Thus, for the sensor failure case, it is not possible to confine $p_{a,i}(s)$ to lie in a fixed direction. Only for fortuitous cases, depending on the dynamics of the system, can this be achieved. However, for any system, the GPV always lies on a hyperplane in the generalized parity space, defined by the vectors E_d^i and B_d^i [10].

The sensor fault isolation can be based on the angle Θ_i, between the GPV and the i^{th} sensor reference hyperplane, SP^i, as illustrated in figure 2. If the i^{th} sensor is faulty, this angle should be zero or less than T_h.

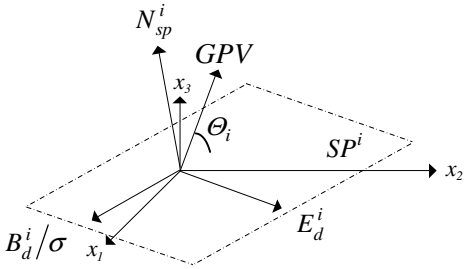

Fig. 2. Sensor FDI

IV. Transformation matrix

The transformation matrix T_r plays an important role in FDI using directional residuals. It is desirable to choose T_r to increase the separation angle between the original set of reference directions and reference hyperplanes as much as possible, to enhance robustness and maximize the number of faults that can be isolated and the number of disturbances that can be decoupled, beyond the number of outputs of the system [6].

This can be formulated as a constrained optimization problem, whose objective is to maximize the angles between the transformed reference directions and reference hyperplanes, to the extent possible. The optimization routine maximizes the minimum of $F_{i,j}(T_r)$, where $F_{i,j}(T_r)$ is the objective function containing the angles between the reference directions and reference hyperplanes that are separable. The mathematical formulation is given by:

$$F_{i,\,j}\,(T_r) = \measuredangle(Z_i\,, Z_j) \tag{11}$$

$$\max_{T_r}\ \min_{\{F_{i,\,j}\}}\{F_{i,\,j}\,(T_r)\} \tag{12}$$

$$such\ that\ c\,(T_r) \leq 0\ ,\ c_{eq}(T_r) = 0$$

where $c(T_r) \leq 0\,, c_{eq}(T_r) = 0$ represent a nonlinear inequality and equality constraints, respectively; and Z_i and Z_j are transformed reference directions, hyperplanes or a combination of both. These directions are given by transforming B_n^j, B_d^i and E_d^i. The high flexibility of the T_r calculation approach proposed using optimization allows us to add different nonlinear constraints to take into account the dynamics of the system and solve some geometrical restrictions. In general, the condition number of T_r should be constrained to be small, to avoid obtaining an ill-conditioned transformation matrix and improve the robustness of the FDI response. For further information on this see [1].

As the number of inputs and outputs in the system increases, the optimization routine to calculate the transformation matrix becomes more challenging since there are more reference directions and reference hyperplanes to separate. For the separator model described in section V, the system has five input and five outputs, which produces 45 different combinations of reference directions, reference hyperplanes and combination of both to be separated in the objective function. Despite the large amount of separation angles to maximize, the original objective function proposed in (11) was capable of calculating a transformation matrix that maximizes the original set of reference directions and reference hyperplanes well enough to provide clear isolation. However, since there are five unparallel hyperplanes, they intersect with each other in a volume, regardless of their separation angle. This condition only affects the FDI performance if the faulty steady-state GPV in a situation where a failure is applied to the i^{th} sensor, GPV_{ss}^i, lies on or close to the hyperplane intersection volume. For simplicity, although the separator FDI is performed in a 5-dimensional space, the hyperplane intersection situation illustrated in fig. 3 is plotted in a 3-dimensional space.

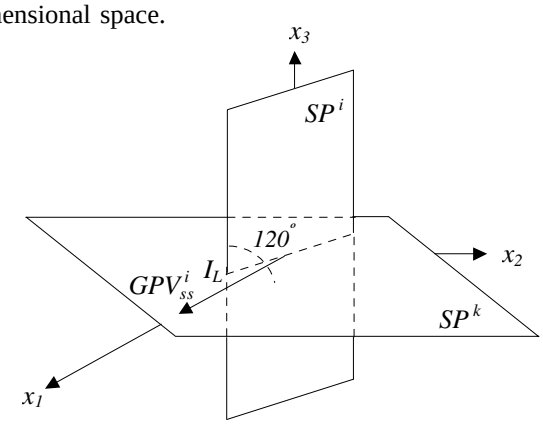

Fig. 3. Planes intersection

Fig. 3 demonstrates that if the GPV_{ss}^i lies on or close to the hyperplane intersection line (I_L), its angle with respect to the i^{th} and k^{th} reference hyperplanes are both zero or close to zero, giving an ambiguous isolation. Nevertheless, this ambiguity can be avoided by adding equation (13) to extend the objective function proposed in (11). This assures that the separation angle between the faulty steady-state GPV for the i^{th} sensor and the k^{th} sensor reference hyperplane is maximized to provide an unambiguous isolation. This can be expressed mathematically as:

$$F_{i,\,j}\,(T_r) = \measuredangle(GPV_{ss}^i\,, Z_k) \tag{13}$$

If equation (13) is omitted during the optimization routine, there is no guarantee that the resulting T_r will not produce a GPV_{ss}^i aligned or close to the i^{th}-k^{th} hyperplanes line intersection. This is illustrated later in section VII, fig. 9. This modification is required only for those cases where the optimization routine using the original objective function in (11) returns a transformation matrix that pushes the faulty steady-state GPV close to a hyperplanes intersection line.

V. Gravity three-phase separation process description

Three-phase separators are designed to separate and remove the free water from the mixture of crude oil and water. The fluid enters the separator and hits an inlet diverter. This sudden change in momentum produces the initial gross separation of liquid and vapor. In most designs, the inlet diverter contains a downcomer that directs the liquid flow below the oil/water interface. This forces the inlet mixture of oil, water and gas to mix with the water continuous phase (i.e., aqueous phase) in the bottom of the vessel and the oil droplets rise to the oil/water interface. This process is called water-washing, and it promotes the coalescence of water droplets which are entrained in the oil continuous phase. The inlet diverter assures that little gas is carried with the liquid. The water wash assures that the liquid does not fall above the gas/oil or oil/water interface, mixing the liquid retained in the vessel and making control of the oil/water interface difficult.

The gas flows over the inlet diverter and then horizontally through the gravity settling section above the liquid. As the gas flows through this section, small drops of liquid that were entrained in the gas and not separated by the inlet diverter are separated out by gravity and fall to the gas-liquid interface. Some of the drops are of such a small diameter that they are not easily separated in the gravity settling section. Before the gas leaves the vessel it passes through a coalescing section or mist extractor to coalesce and remove them before the gas leaves the vessel.

The simulation model basically consists of two processes, as illustrated in figure 4. The first is a two-phase separator in which hydrocarbon fluids from oil wells are separated into two phases to remove as much light hydrocarbon gases as possible. The produced liquid is then pumped to the three-phase separator (i.e., the second process), where water and solids are separated from oil. The produced oil is then

pumped out and sold to refineries and petrochemical plants if it meets the required specifications.

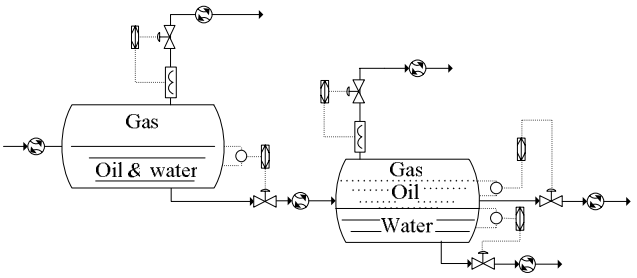

Fig. 4. Gravity three-phase separator process

The two separation processes of the simulation model are controlled to maintain the operating point at its nominal value, and to minimize the effect of disturbances on the produced oil's quality. As shown in figure 4, the first separation process is controlled by two PI controller loops. In the first loop, the liquid level is maintained by manipulating the liquid outflow valve. The second loop is to control the pressure inside the two-phase separator by manipulating the amount of the gas discharge. The second separation process has three PI controller loops. An interface level PI controller maintains the height of the oil/water interface by manipulating the water dump valve. While the oil level is controlled by the second PI controller through the oil discharge valve, the vessel pressure is maintained constant by the third PI loop [11].

VI. System identification

Chemical processes are inherently nonlinear in nature, making it very difficult and even impractical to develop an accurate mathematical model for the system. This has been one of the main reasons that has limited the application of quantitative model-based FDI techniques in real industrial processes [3].

In order to address this issue for the GPV approach, a system identification module is implemented for the gravity three-phase separator described in section V. It is assumed that the actual nonlinear model for the plant is not available and also the system order is unknown, thus the analytical linearized state-space representation cannot be obtained. The only available information is input-output data corresponding to pseudo-random binary sequences (PRBS) applied as setpoint variations to excite each of the system reference inputs [12]. System identification is performed using the standard prediction error/maximum likelihood method *(pem)* implemented in MATLAB®, which provides a linearized state space model. Since the model order is not specified, this is calculated automatically using the subspace-based method *(n4sid)*, to provide the best fitting. The first 600 input-output samples are used to identify the model, while the last 300 samples are used to validate it. Fig. 5 shows the

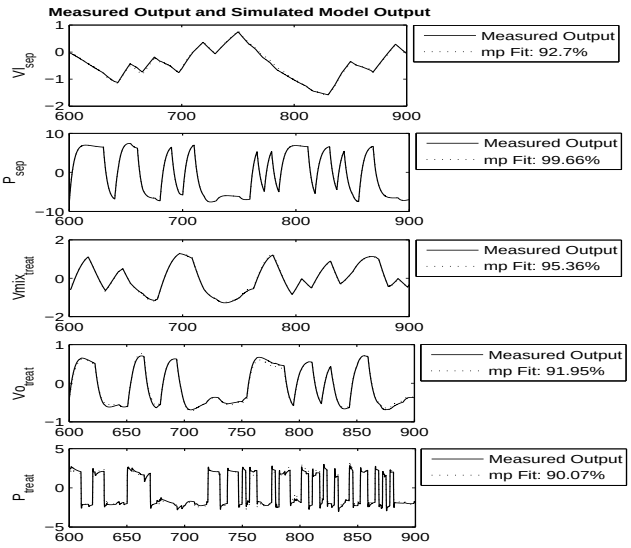

Fig. 5. Three-phase separator system identification

excellent system identification validation results for each output variable.

Because of the highly nonlinear nature and complexity of the process, the "best model order" obtained during the identification process is 10, which is considerably higher than the actual order of five. However, the identified linearized 10^{th} order state space model provides a highly satisfactory % of fitting overall, as shown in fig. 5. Also, this order discrepancy allows us to test the GPV technique using a state space model whose state variables do not correspond to physical parameters as in the original nonlinear model. This matter is discussed in more detail in section VII.

VII. Fault detection and isolation results

Using the identified linearized 10^{th} order state-space model discussed in section VI, fault detection and isolation using the GPV technique is performed for different sensor and actuator fault scenarios. First, a -50% bias fault is applied to the treator vapor outflow valve (denoted fault F10) at the nominal operating point. Fig. 6 shows the GPV magnitude and its corresponding sensor and actuator angles. It is observed that right after the fault is applied at t=300 sec, the GPV magnitude increases significantly allowing a definite and fast detection. Also, the GPV angle corresponding to actuator fault F10 moves toward zero, while keeping a minimum separation of approximately 10 degrees with the other reference directions. Thus, the detection and isolation are fast and clear, which are important features for FDI.

Fig. 7 shows the FDI results for a -50% bias fault applied to the separator vapor outflow valve (fault F7), for a setpoint variation of 10%. It is observed that even for a significant setpoint variation, the GPV magnitude and angle can detect and isolate the fault promptly and clearly.

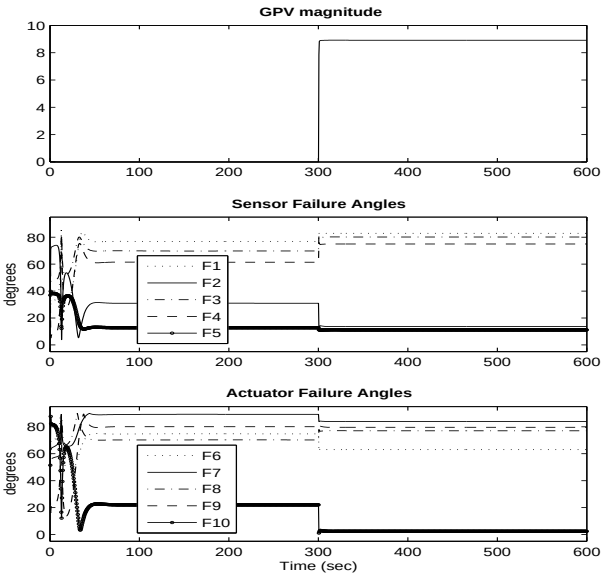

Fig. 6. FDI results for actuator 10 fault

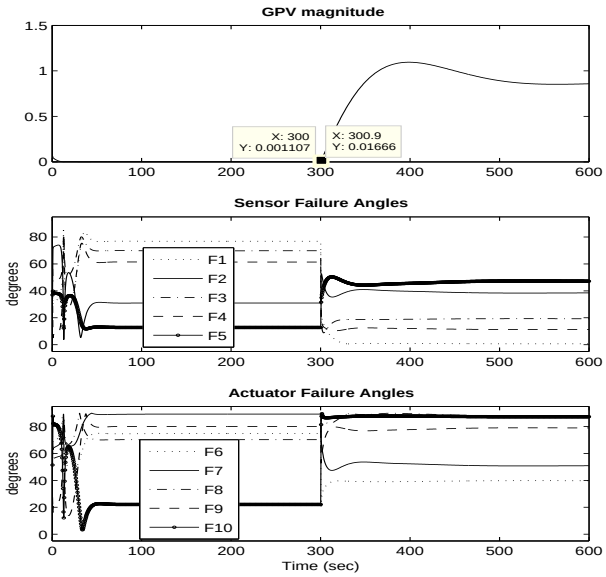

Fig. 8. FDI results for sensor 1 fault - Modified

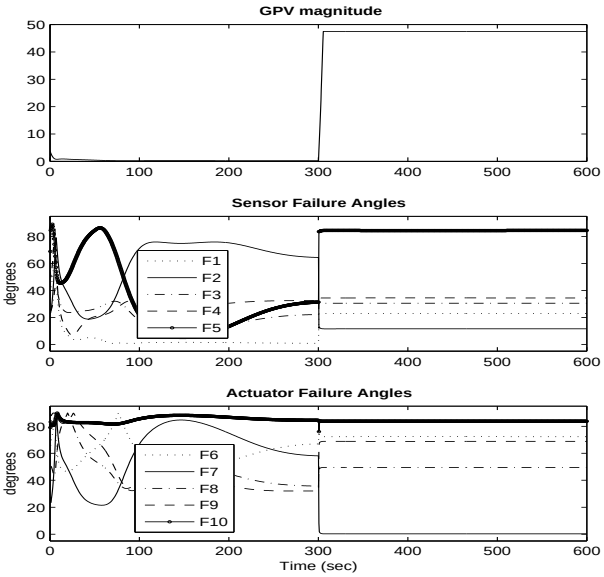

Fig. 7. FDI results for actuator 7 fault

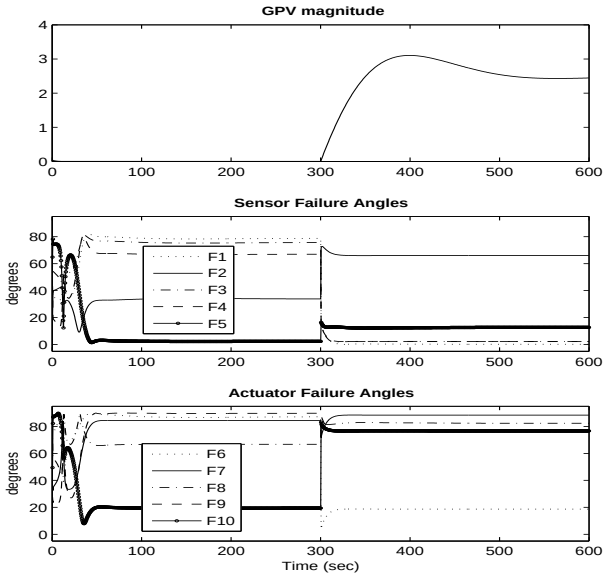

Fig. 9. FDI results for sensor 1 fault - Unmodified

For the sensor case, a ramp fault with a slope of 0.4 representing an inaccurate sensor reading increasing with time is applied to the separator liquid volume sensor (fault F1) at the nominal operating point. The FDI results illustrated in fig. 8 show that even for faults slowly increasing with time, the GPV magnitude increases around 15 times, only 0.9 sec after the fault is applied at t=300 sec, providing immediate detection. Also, the GPV angle corresponding to sensor 1 (F1) moves toward zero very rapidly reaching a minimum separation of around 10 degrees with the other reference directions within the first 20 sec. These detection and isolation times are acceptable, since the fault was applied to the liquid phase which has slower dynamics than the gas phase.

However, if the modification to the objective function described in section IV equation (13) is omitted, the GPV_{ss} lies very close to the intersection volume for hyperplanes 1, 3 and 4, giving an isolation angle close to zero for all of them. This is illustrated in fig. 9, where the angles corresponding to F1, F3 and F4 are all close to zero, making the isolation ambiguous.

Fig. 10 shows the FDI results when the treator oil volume

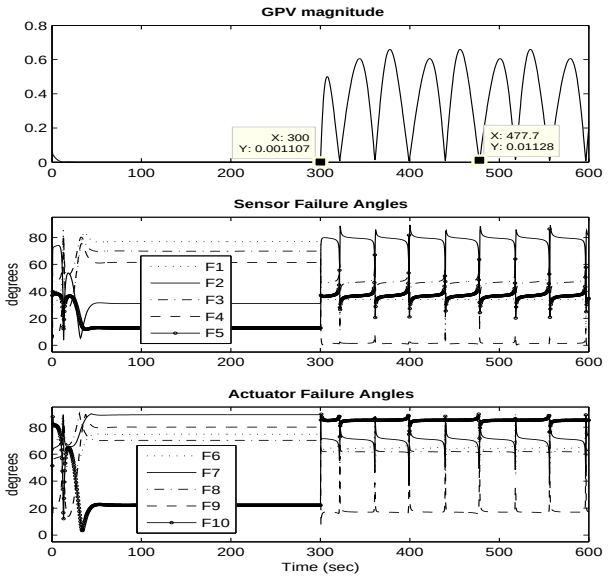

Fig. 10. FDI results for sensor 4 fault

sensor signal is contaminated by a 20% sinusoidal interference with a single frequency of 12.73 mHz (i.e., reading from a wireless sensor). If the magnitude threshold T_{hm} is set to be small, for instance 4 times the fault free GPV magnitude, the fault is detected continuously after $t_{fault} = 300\ sec.$ However, the isolation is ambiguous periodically for approximately 300 milliseconds due to the GPV angles behaviour during the spikes caused by the $|GPV|$ minimums.

From the previous FDI results obtained for sensors and actuators when different type and size of faults are applied it is seen that the GPV technique works satisfactory using the 10^{th} order state-space model computed by system identification. This demonstrates that the state-space representation used in the left coprime calculations in equations (4) and (5) are not required to match either the actual system order or the physical state variables of the original nonlinear system. Also, despite the fact that the identified model did not provide an ideal % of fitting for all the outputs, as it is shown in the separator identification results illustrated in fig. 5, this did not affect the GPV performance. Clarifying these aspects demonstrates that the GPV technique is feasible for implementation in real industrial processes even when mathematical models are not available.

VIII. CONCLUSIONS

The GPV technique has been successfully tested on a larger scale industrial process in the absence of a mathematical model, by incorporating a system identification module. This has demonstrated that the state-space representation does not require the actual system order and/or physical states to provide suitable left coprime factors for the GPV computation. Thus FDI is possible even for those systems where input-output data is the only accessible information. Also, the state-space flexibility offers the possibility of applying state-space transformations for those cases where the linearized mathematical model is available but exhibits some inseparable reference directions and/or rank-deficient matrices. The hyperplanes intersection problem has been clarified and solved by extending the objective function during the optimization routine to compute the transformation matrix.

IX. ACKNOWLEDGMENTS

This project is supported by Atlantic Canada Opportunities Agency (ACOA) under the Atlantic Innovation Fund (AIF) program. The authors gratefully acknowledge that support and the collaboration of the Cape Breton University (CBU), the National Research Council (NRC) of Canada, and the College of the North Atlantic (CNA).

REFERENCES

[1] M. Omana and J. H. Taylor, "Robust Fault Detection and Isolation Using a Parity Equation Implementation of Directional Residuals", *Proc. IEEE Advanced Process Control Applications for Industry Workshop (APC2005)*, 2005.

[2] M. Omana and J. H. Taylor, "Enhanced Sensor/Actuator Resolution and Robustness Analysis for FDI Using the Extended Generalized Parity Vector Technique", *Proc. American Control Conference*, Minneapolis, MN, 2006.

[3] V. Venkatasubramanian and R. Rengaswamy and K. Yin and S. N. Kavuri, A Review of Process Fault Detection and Diagnosis, part III: Process History Based Methods, *Computers and chemical engineering*, vol. 27, 2003, pp 327-346.

[4] V. Venkatasubramanian and R. Rengaswamy and K. Yin and S. N. Kavuri, A Review of Process Fault Detection and Diagnosis, part I: Quantitative Model-Based Methods, *Computers and chemical engineering*, vol. 27, 2003, pp 293-311.

[5] F. Hamelin and D. Sauter and M. Aubrun, "Fault Diagnosis in Systems using Directional Residuals", *Proceedings on the 33rd IEEE Conference on Decision and Control*, 1994.

[6] J. J. Gertler and R. Monajemy, Generating Directional Residuals with Dynamic Parity Relations, *Automatica*, vol. 31, no. 4, 1995, pp 627-635.

[7] J. J. Gertler, *Fault Detection and Diagnosis in Engineering Systems*, Marcel Dekker, Inc., 1998.

[8] P. J. Antsaklis, Proper Stable Transfer Matrix Factorization and Internal System Descriptions, *IEEE Transactions on automatic control*, vol. AC-31, no. 7, 1986, pp 634-638

[9] M. Vidyasagar, *Control System synthesis: A Factorization Approach*, The MIT press, 1985.

[10] N. Viswanadham and J. H. Taylor and E. C. Luce, A frequency domain approach to failure detection and isolation with application to GE-21 turbine engine control systems, *Control-Theory and advanced technology*, vol. 3, no. 1, 1987, pp 45-72.

[11] A. F. Sayda and J. H. Taylor, "Modeling and control of three-phase gravity separators in oil production facilities", *Proc. American Control Conference*, New York, NY, 2007.

[12] Y. Zhu, *Multivariable system identification for process control"*, Pergamon, 2001.

[13] E. Y. Chow and A. S. Willsky, Analytical Redundancy and the Design of Robust Failure Detection Systems, *IEEE Transactions on automatic control*, vol. AC-29, no. 7, 1984, pp 603-614.

[14] J. J. Gertler, Fault detection and isolation using parity relations, *Control Eng. Practice*, vol. 5, no. 5, 1997, pp 653-661.

[15] J. J. Gertler, Survey of Model-Based Failure Detection and Isolation in Complex Plants, *IEEE Control Systems Magazine*, vol. 8, no. 4, 1988, pp 3-11.

[16] A. S. Willsky, A survey of design methods for failure detection in dynamic systems, *Automatica*, vol. 12, no. 6, 1984, pp 601- 611.

[17] J. J. Gertler and D. Singer, A new structural framework for parity equation-based failure detection and isolation, *Automatica*, vol. 26, no. 2, 1990, pp 381-388.